PNAS
www.pnas.org

Supplementary Information for

Robust paths to net greenhouse gas mitigation and negative emissions *via* advanced biofuels

John L. Field, Tom L. Richard, Erica A. H. Smithwick, Hao Cai, Mark S. Laser, David S. LeBauer, Stephen P. Long, Keith Paustian, Zhangcai Qin, John J. Sheehan, Pete Smith, Michael Q. Wang, and Lee R. Lynd

Corresponding author: John L. Field
Email: John.L.Field@gmail.com

This PDF file includes:

www.pnas.org/cgi/doi/10.1073/pnas.1920877117

Ecosystem carbon accounting conventions

We used the metric of net ecosystem carbon balance (NECB) as defined in Chapin *et al.* 2006 (1), and equations presented in Lovett *et al.* 2006 (2) to represent changes in ecosystem carbon storage over time. It is common for bioenergy greenhouse gas (GHG) accounting studies to focus on soil organic matter (SOM) as the primary indicator of long-term changes in ecosystem carbon storage. In conventional agricultural systems SOM is the largest, most stable, and most integrative carbon pool, whereas carbon in surface vegetation and litter is often ignored as a smaller and more transient pool that fluctuates greatly over the course of a growing season (3). However, the current analysis considered more extensive land use changes including reforestation and grassland restoration, and thus required more extensive ecosystem carbon accounting capable of representing changes in aboveground woody and herbaceous biomass in addition to belowground storage.

Assuming that there are no significant inputs or outputs of *inorganic* carbon in our agricultural and forested systems of interest, we used Eqns. 2 & 3 from reference (2) to represent a simple mass balance for *organic* carbon:

$$\Delta C_{org} = GPP + I - R_e - Ox_{nb} - E$$

where changes in ecosystem organic carbon storage reflect the balance between organic carbon inputs from gross primary production (GPP, the total rate of C fixation by photosynthesis) and other inputs (I), and losses from ecosystem respiration (R_e, the sum of autotrophic respiration R_a and heterotrophic respiration R_h), non-biotic oxidation of organic carbon due to fire and ultraviolet oxidation (Ox_{nb}), and other exports of carbon from the system (E).

The total change in ecosystem organic carbon storage is equivalent to NECB in systems where inorganic carbon fluxes are negligible, as per Eqn. 1 in reference (1). This change can be further divided into aboveground (ΔC_{AG}) and belowground (ΔC_{BG}) components for accounting convenience. We assumed that lateral inputs of organic carbon from outside the boundary of our agricultural and forested systems are minimal, that losses from fire and non-biotic oxidation are negligible, and that the only significant export of organic carbon from our systems is harvest of biomass (Harv). We therefore simplified our governing equation to:

$$NECB = \Delta C_{AG} + \Delta C_{BG} = GPP - R_e - Harv$$

GPP in terrestrial ecosystems is typically evaluated via eddy flux towers or other direct gas exchange measurements. However, DayCent and many other ecosystem models simulate net primary production, the difference between GPP and autotrophic respiration (NPP=GPP–R_a). We therefore re-wrote our ecosystem carbon storage governing equation for better compatibility with ecosystem model outputs as:

$$NECB = \Delta C_{AG} + \Delta C_{BG} = NPP - R_h - Harv$$

Integrating these carbon balance estimates over large spatial and temporal scales in order to account for landscape heterogeneity, disturbance, and interactions between the two is often termed net biome production (NBP) (1). NBP has been used previously to estimate spatially continuous long-term forest carbon storage trends at regional scales where inventory data is plentiful (4). However, our analysis was spatially discreet, and thorough accounting for different possible future disturbance regimes was outside the scope of the current work.

Reforestation terminology

The terms ‘reforestation’ and ‘afforestation’ are often invoked together or used interchangeably, and their technical definitions across the scientific and regulatory literature are varied and highly overlapping (5). Our analysis considered bioenergy production as an alternative to lightly-managed or unmanaged restoration of natural vegetation on former agricultural land, for example the historical abandonment of cropland in New England or more recent establishment of conservation easements on marginal or degraded land. Many of the definitions cited in reference (5) and other papers cited in our work (e.g., reference (6)) would use the term afforestation for such cases, as these lands were put into agriculture long ago and have not recently been classified as forest. However, in the context of climate mitigation and carbon dioxide removal the term afforestation is often invoked for the highly-managed establishment of forest on lands that were not previously forested, with the explicit goal of sequestering carbon (7). This can involve intensive site preparation or application of fertilizer or irrigation to promote tree establishment, and/or the planting of non-native higher-productivity species to increase sequestration rates. Such schemes can produce high initial rates of carbon sequestration, though at the expense of less biodiversity value and possibly reduced resilience to future disturbance (8).

Our mitigation-focused analysis considered secondary succession of regionally appropriate forest types, and as such we used the term reforestation to differentiate from that more targeted, active forest establishment and management for carbon sequestration (7). The ultimate biophysical mitigation potential of such active afforestation depends on tree selection, management choices, and the vulnerability of the resulting system to wildfire and other natural disturbances. A thorough analysis and quantification of these factors was outside the scope of the current work. Rather, our case study sites were selected to be representative of reforestation following agricultural abandonment in regions where forest was historically the dominant land cover (Wayne County, New York) or within the historic forest–grassland transition zone (Webster County, Iowa, and La Salle Parish, Louisiana) where both land covers would have been common and disturbance frequent. These sites also avoid boreal and montane forests in which countervailing biophysical warming effects (e.g., albedo increases) may offset much of the climate mitigation value of carbon sequestration (9).

DayCent simulation post-processing

DayCent estimates NPP as a dynamic function of insolation (based on latitude and weather conditions), soil temperature and moisture, canopy development (affects light interception), soil mineral nitrogen availability, and root zone development (affects ability of plant to access moisture and nitrogen in deeper soil layers) (10). Carbon partitioning between shoots and roots is dynamically adjusted based on simulated plant moisture and nutrient stress status. Soil organic carbon (SOC) dynamics reflect the rate of carbon inputs from aboveground litter and fine root turnover, and their transfer between three conceptual SOC pools (‘active’, ‘slow’, and ‘passive’) with different intrinsic turnover times. Actual turnover rates are dynamically adjusted for soil moisture and temperature conditions, and carbon stabilization efficiency is determined as a function of soil texture and plant litter chemistry. Nitrogen transformations simulated include N fixation, mineralization and immobilization, volatilization, leaching, ammonification,

nitrification, and denitrification. Losses in the form of nitrous oxide (N_2O) are controlled by mineral N availability, organic carbon content, water-filled pore space (in turn affected by climate and soil texture), and soil pH.

We post-processed our DayCent simulation results for this assessment as follows:

***Harvest*—**Harvested herbaceous and woody biomass carbon amounts are reported via the 'crmvst' and 'tcrem' parameters of the DayCent list.100 output, respectively. These parameters are reported on an annual basis and were summed and translated to a daily time-step series within our analysis code. Our switchgrass simulations assumed harvest of 95% of total aboveground switchgrass biomass, with the remaining 5% left on the field as surface litter. Our secondary forest clear-cutting scenarios assumed harvest of all live stems and branches and burning of all remaining foliage and dead downed stems and branches.

***Ecosystem carbon storage*—**The size of various above- and belowground carbon pools is reported in the dc_sip.csv model output on a daily time step. Note that DayCent models crop and grass growth with one set of non-soil carbon pools, and forest growth with another. Our analysis code calculated intermediate carbon pool sizes as well as total above- and belowground ecosystem carbon across both the both crop/grass and forest pools each day, as summarized in Table S3. DayCent output is in units of g C m^{-2} y^{-1}, which our code then converted to both a Mg C ha^{-1} y^{-1} basis and a Mg CO_2e ha^{-1} y^{-1} basis. Average annual NECB (and its above- and belowground constituents) over the first 30 years of simulation was evaluated in this manner for Figs. 1 and 4 in the main manuscript.

***Net primary production & heterotrophic respiration*—**Simulated daily NPP is reported in the dc_sip.csv model output, which we then converted to a Mg C ha^{-1} y^{-1} basis. Daily heterotrophic respiration (R_h) was calculated by difference from DayCent-simulated NPP, NECB, and harvest results using Eqn. [1] in the Methods section of the main manuscript.

***Nitrous oxide*—**Simulated daily N_2O emissions from soil nitrification and denitrification processes are reported individually in the DayCent nflux.out output in units of g N ha^{-2}. Our analysis code summed these two sources and converted the result to a Mg CO_2e ha^{-1} basis. Simulated N_2O emissions were relatively small, and thus were combined with the bioenergy supply chain (BSC) emissions term to simplify the display of Fig. 4 in the main manuscript.

Figures S7–9 provide an illustrative example of simulated changes in above- and below-ground carbon storage after retirement of Iowa cropland and conversion to native forest types, grassland, or cultivation of current-day switchgrass, a disaggregation of select results underlying Fig. 1 in the main manuscript. The definitions of the individual carbon pools shown are summarized in Table S3.

DayCent forest calibration

We created regionally specific parameterizations to simulate native forest growth at the different case study sites based on the forest yield tables reported in Smith *et al.* 2006 (6), which are derived from US Forest Service inventory data and models. That reference includes forest yield tables describing changes in stand carbon density for both forest growth following clearcut harvest of prior existing forest [reference (6), Appendix A] and for new forest growth on land previously under other land cover (Appendix B). Those

two cases have the same carbon density values for live trees, standing dead trees, and understory vegetation, but the 'forest-following-forest' case (Appendix A) includes high initial levels of down dead wood and forest floor litter, and the 'new-forest' case (Appendix B) has lower initial soil carbon.

Our DayCent calibration consisted of an automated ensemble approach based on six combinations of SSURGO soil and NARR weather selected at random from the full range present within each case study county. We performed model spin-up for both 'forest-following-forest' and 'forest-following-crop' (comparable to 'new-forest') cases to align with the yield tables in reference (6), Appendix A and B, respectively. We then simulated forest regrowth for each element of both ensembles, calculated total living and dead biomass C density on an annual time step (Table S4), and computed the average values across each ensemble. We ensured a conservative comparison for our bioenergy scenarios by calibrating DayCent's forest productivity potential and symbiotic nitrogen fixation to match total (live + dead) stand carbon density for the most productive forest type within each relevant region in reference (6) from stand age 0–85 years, bringing the DayCent-simulated results as close as possible to—but not below—the target values. We used the 'Northeast' region in reference (6) to represent our New York case study, the 'Northern Prairie States' region to represent our Iowa case study, and the 'South Central' region to represent our Louisiana case study.

Nitrogen inputs from atmospheric deposition and symbiotic nitrogen fixation are an important control on successional forest productivity, though afforestation/reforestation soil nitrogen dynamics are highly variable and difficult to generalize (11–13). Leaving DayCent atmospheric deposition inputs at their default values, we adjusted symbiotic nitrogen fixation for broad consistency with soil total nitrogen trend data from two representative afforestation studies (14, 15) and to minimize divergence between the forest-following-forest and forest-following-crop ensembles due to differing site fertility conditions (i.e., different initial soil organic matter levels). Finally, we adjusted tree tissue mortality so the forest-following-crop ensemble dead biomass carbon densities would best match the corresponding values in reference (6), Appendix A. Note that forest floor (i.e., surface litter) and soil organic carbon were excluded from the comparison, as DayCent models these quantities in a more explicit manner than does reference (6). Final forest calibration results are detailed in Fig. S10.

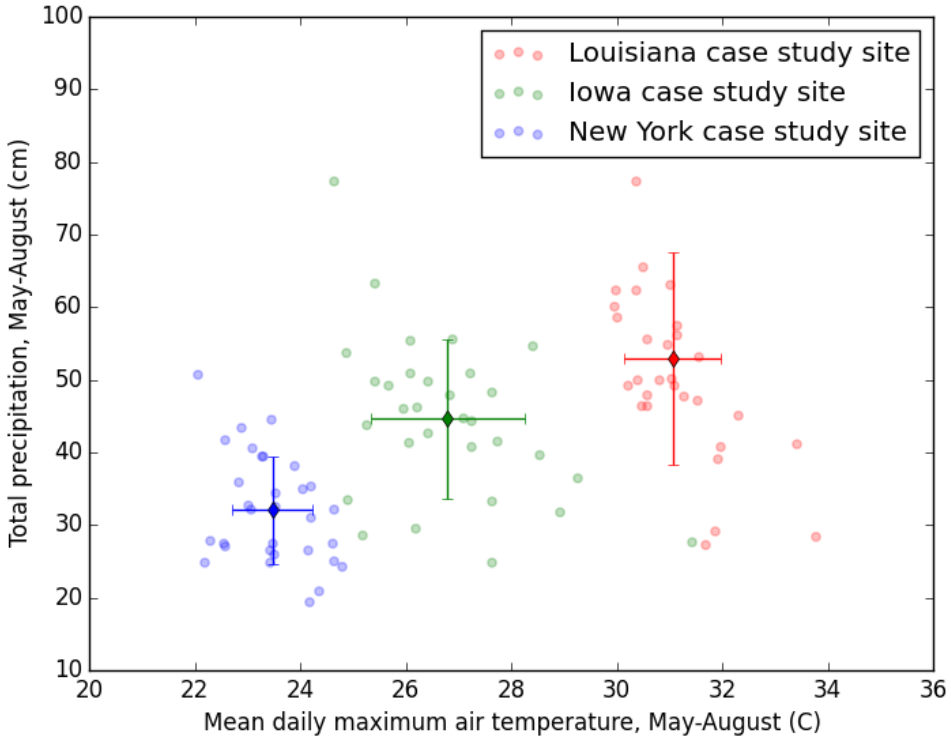

Fig. S1. Comparison of growing season temperature and precipitation at the three case study sites. Based on the North American Regional Reanalysis data (16). Points show records for individual years in the 1979–2009 record. Diamonds indicate inter-annual means, with error bars showing one standard deviation.

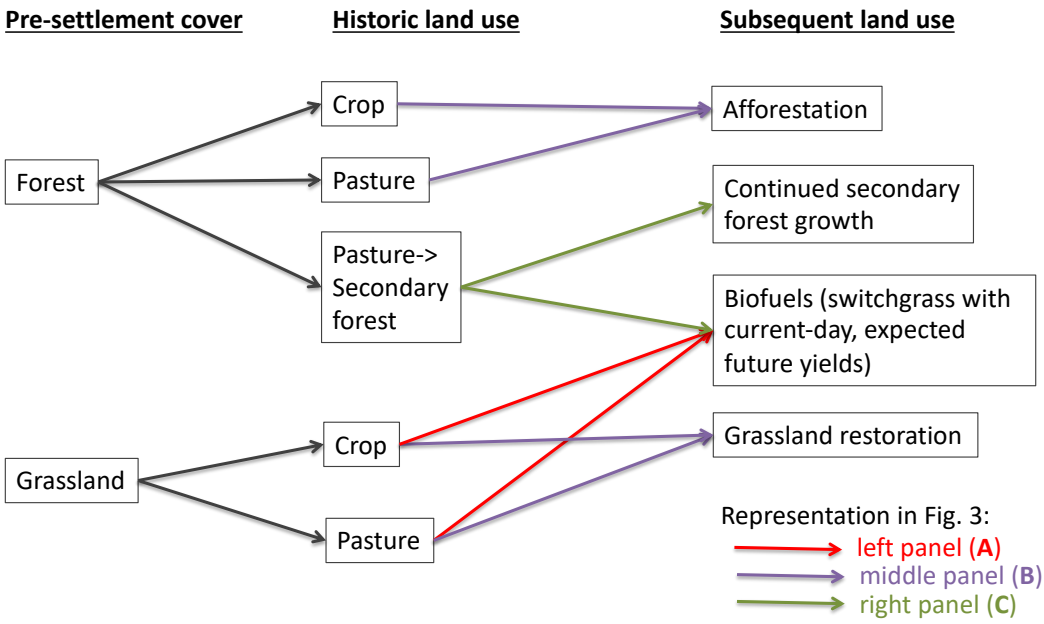

Fig. S2. DayCent simulation scenario matrix. Model initialization requires representation of pre-settlement land cover and historic land use. Arrow colors show which scenarios are included in which panel of Fig. 3 of the main manuscript, as indicated in the key.

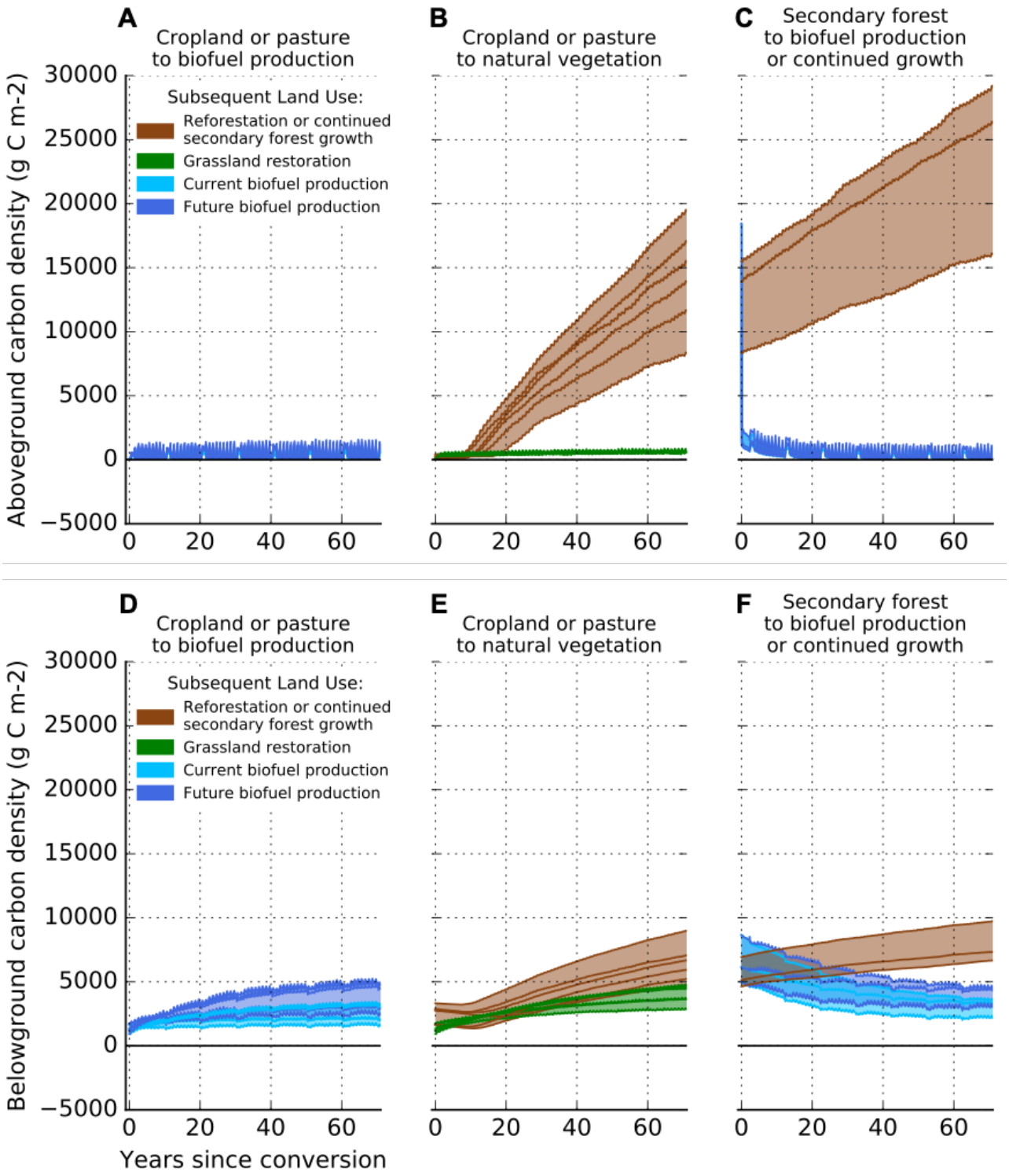

Fig. S3. Cumulative above- (A, B, C) and below-ground (D, E, F) NECB versus time. Results plotted individually for scenarios of (**A, D**) biofuel production on former agricultural land, (**B, E**) natural vegetation restoration on former agricultural land, and (**C, F**) secondary forest harvest and conversion to biofuel production versus continued undisturbed growth, evaluated at the three case study sites.

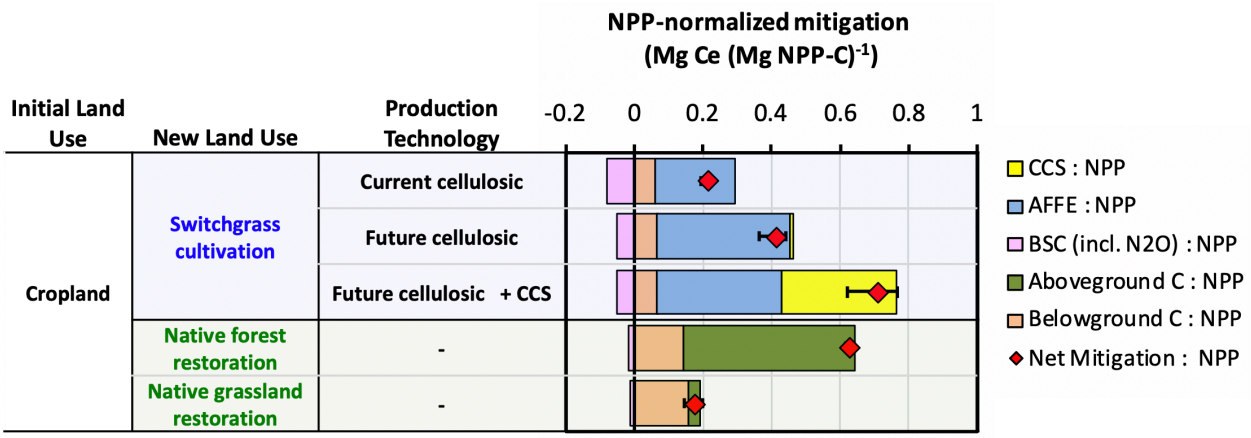

Fig. S4. NPP-normalized mitigation shares. Results for bioenergy and vegetation restoration scenarios on former cropland re-factored in units of metric tonnes of carbon equivalent (Mg Ce) mitigated per tonne of NPP carbon (Mg NPP-C) fixed. This illustrates the relative effectiveness of different scenarios at storing biogenic carbon and/or mitigating fossil energy emissions per unit of plant productivity, independent from the differences in plant productivity between scenarios.

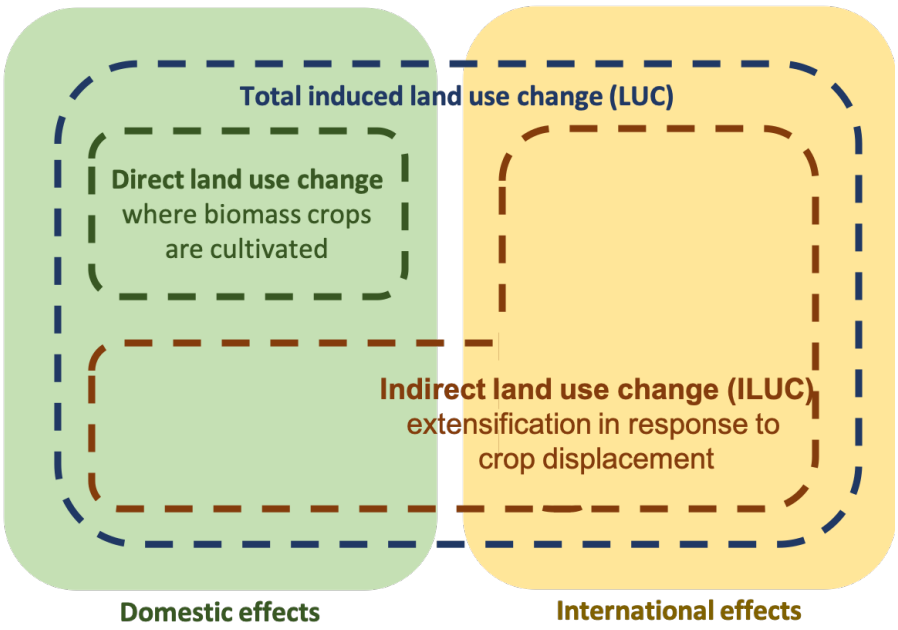

Fig. S5. Land use change emissions. This conceptual diagram illustrates the difference between direct land use change, the domestic and international components of indirect land use change (ILUC), and total induced LUC as the sum of all direct and indirect land use change effects combined.

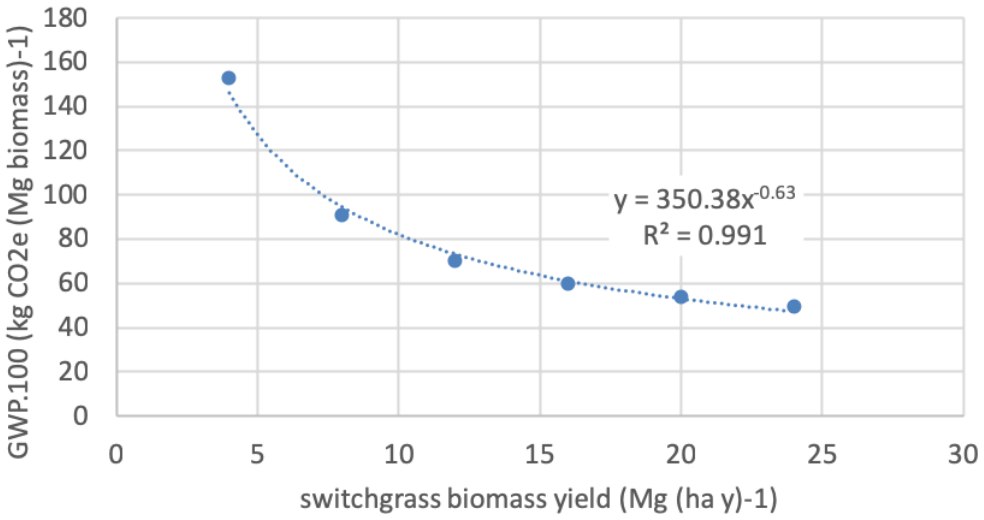

Fig. S6. Farm–to–biorefinery-gate GHG footprint of switchgrass biomass as a function of yield. Includes farm inputs and energy use, biomass harvest, and farm–biorefinery transport. Excludes changes in soil carbon and soil nitrous oxide emissions.

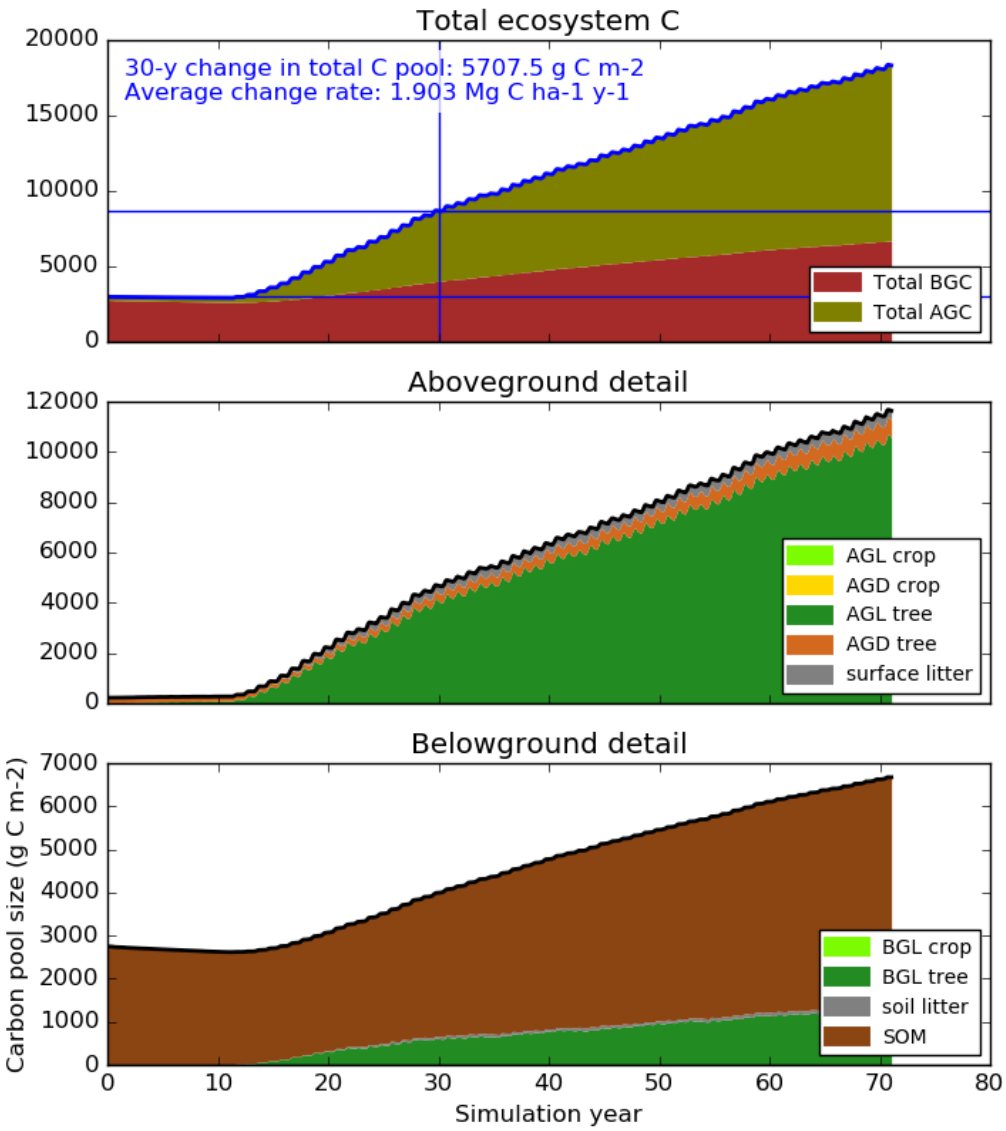

Fig. S7. DayCent simulation detail for reforestation on former Iowa cropland. Change in NECB over time (top panel) and associated above- and belowground carbon pool detail (middle and lower panel, respectively), with pools defined as per Table S3. Calculation of the 30-year average annual NECB is illustrated with blue lines. In this scenario, most of the increase in ecosystem carbon storage is due to aboveground live (AGL) biomass (specifically tree stems, branches, and foliage, shown in dark green in the middle panel).

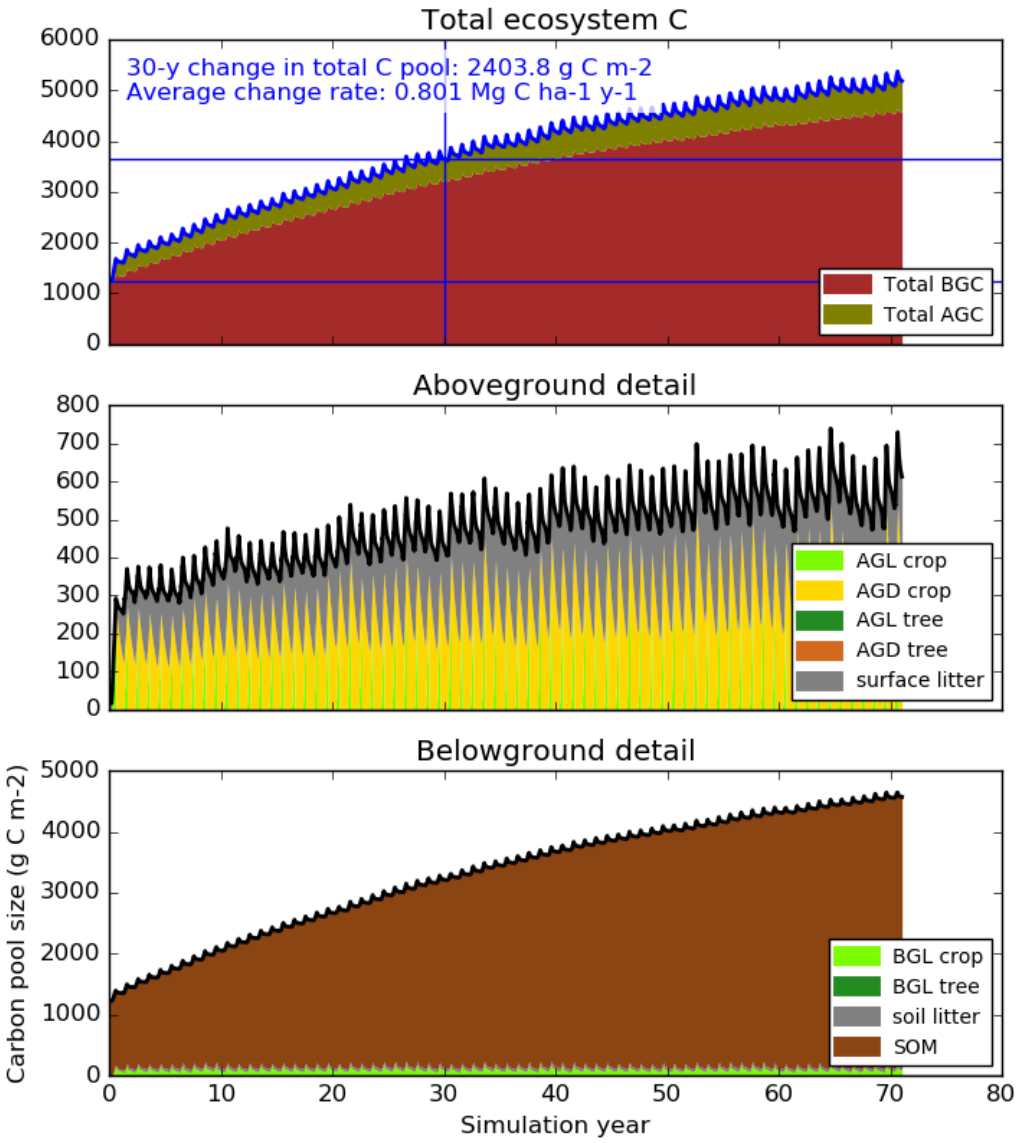

Fig. S8. DayCent simulation detail for grassland restoration on former Iowa cropland. Note the changes in y-axis scaling from the previous figure. Compared to the previous reforestation scenario, soil organic matter (SOM) carbon increases by a similar amount over the course of the grassland restoration simulation, but aboveground carbon storage remains modest, dominated by standing aboveground dead (AGD) biomass and surface litter (yellow and grey colors in the middle panel). The saw-tooth pattern in total aboveground carbon is driven by the grass growing season between spring green-up and fall senescence.

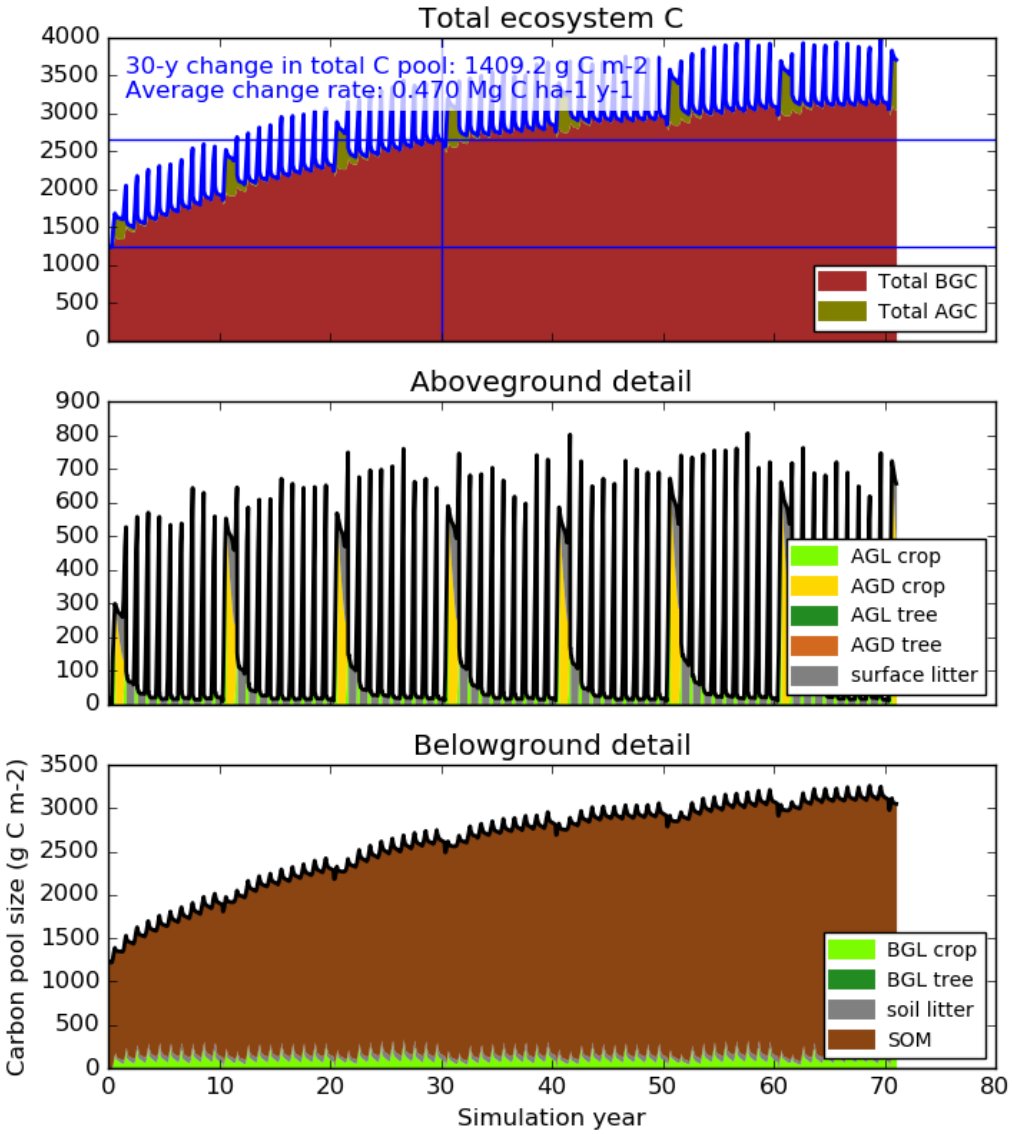

Fig. S9. DayCent simulation detail for current-day switchgrass production on former Iowa cropland. Note the changes in y-axis scaling from the previous figure. The fluctuation in aboveground dead (AGD) crop biomass every 10 years is due to stand replanting (switchgrass not harvested the year of planting). Compared to the previous grassland restoration scenario, soil carbon increase is more modest due to removal of aboveground biomass during harvest and the subsequent lack of surface litter as an input to SOM formation. However, simulated productivity is much higher due to management (fertilizer application that relieves nitrogen limitations on growth) and lack of self-shading from accumulated standing dead biomass.

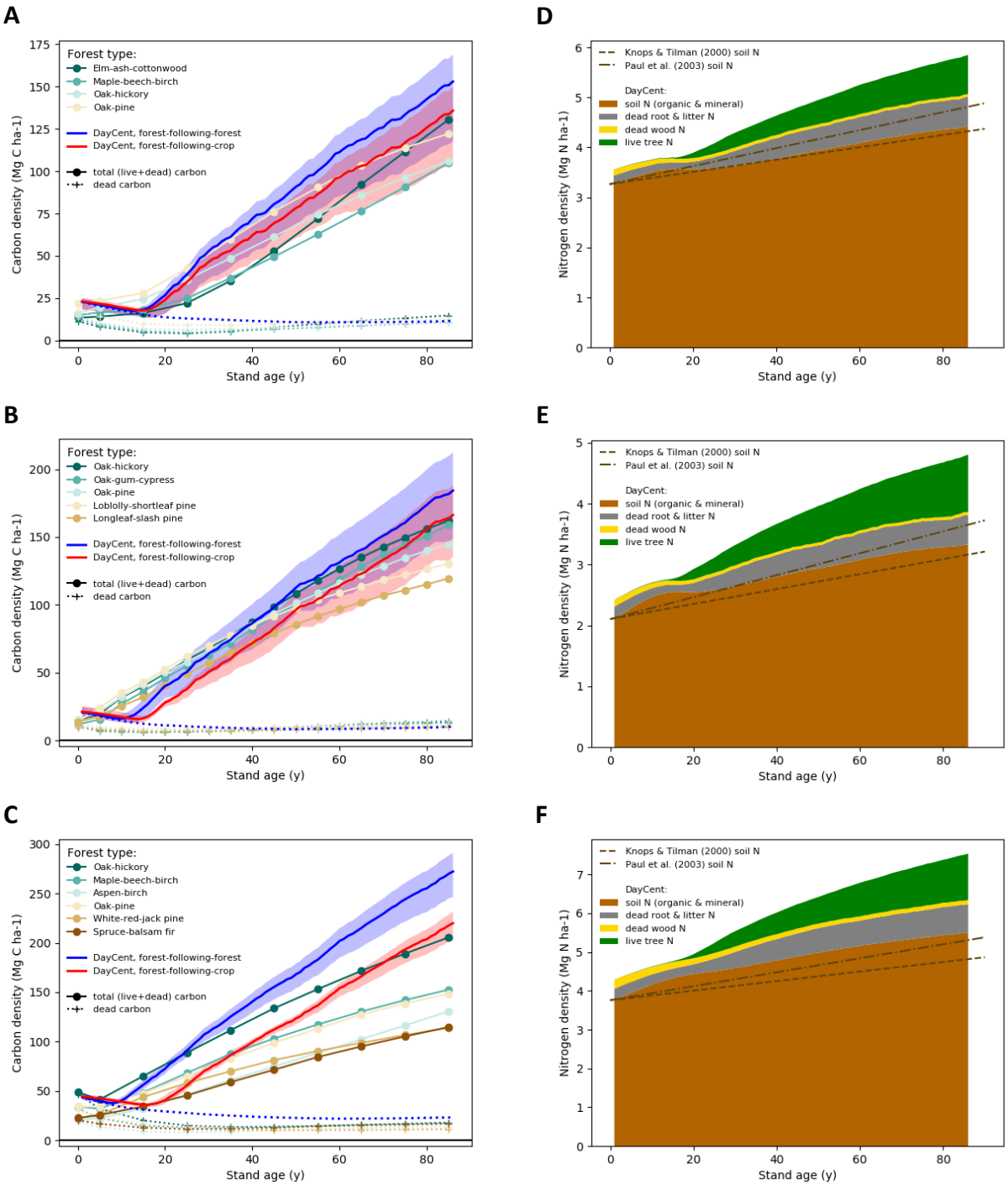

Fig. S10. DayCent forest calibration detail. Showing stand carbon and nitrogen density results, respectively, for the Iowa (**A** and **D**), Louisiana (**B** and **E**), and New York (**C** and **F**) case study sites, as compared to calibration targets. For the carbon plots **A–C**, different forest types are shown in different shades of blue to brown, with dead carbon shown with plus-sign markers and dotted lines, and total stand carbon shown with circular markers and solid lines. Corresponding DayCent simulation results are shown in red (forest-following-crop) and blue (forest-following-forest). The nitrogen plots **D–F** show the trend in total soil N (both organic & inorganic) in comparison to the rates measured by Knopps & Tilman (ref. 14) and Paul *et al.* (ref 15), along with other simulated N pools.

Table S1. Detailed ecosystem & biorefinery modeling results (30-year simulation averages).

	Current biofuels	Future biofuels	Future biofuels+ CCS	Grassland restoration	Reforestation
Ecosystem performance					
NPP (Mg C ha^{-1} y^{-1})	8.7 (7.0–11.7)	14.2 (11.3–19.0)		4.9 (3.4–6.9)	3.7 (1.8–5.0)
NECB (Mg C ha^{-1} y^{-1})	0.32 (0.11–0.60)	0.63 (0.33–1.06)		0.71 (0.54–1.00)	2.3 (1.0–3.4)
NECB:NPP ratio	0.04 (0.01–0.07)	0.05 (0.02–0.07)		0.15 (0.09–0.22)	0.61 (0.55–0.66)
Harvest (Mg C ha^{-1} y^{-1})	5.7 (5.0–6.7)	9.3 (8.2–11.0)		NA	
Harvest:NPP ratio	0.67 (0.57–0.72)	0.67 (0.58–0.73)			
Yield[a] (Mg dry biomass ha^{-1} y^{-1})	11.5 (10.2–13.5)	18.4 (16.2–21.8)			
Biorefinery performance					
Energy efficiency[b]	**43.3%**	**71.2%**	**67.6%**		
Ethanol	40.4%	54.1%	54.1%		
FT liquids	NA	15.8%	15.8%		
Electricity	3.0%	1.3%	-2.3%		
Fraction biomass C in fuel	**26.3%**	**46.1%**	**46.1%**		
Fraction biomass C emitted at biorefinery	**73.7%**	**52.2%**	**4.1%**		
Fraction biomass C sequestered via CCS or char	**0%**	**1.7%**	**49.8%**		
CCS + char sequestration rate (Mg C ha^{-1} y^{-1})	**NA**	0.13 (0.12–0.15)	4.8 (4.2–5.7)		
(CCS+char):NPP ratio	**NA**	0.009 (0.008–0.010)	0.34 (0.30–0.37)		

[a]based on the cellulosic biomass chemical composition specified in reference (17)
[b]energy content of biorefinery products as a fraction of input dry feedstock lower heating value

Table S2. Detailed ecosystem & biorefinery modeling results (30-year simulation averages).

Feedstock	**Switchgrass**					**Miscanthus**			**Perennial grasses**
Model	FASOM -FAPRI	GTAP 1	GTAP 2	GTAP 3 CCLUB	GCAM	GTAP 1	GTAP 2	GTAP 3 CCLUB	GLO-BIOM
Reference	(18)	(19, 20)	(19, 21)	(19, 22)	(23)	(19, 20)	(19, 21)	(19, 22)	(24)
Reported total induced LUC (g CO_2e MJ^{-1})	13.4	2.7[a]	8.9[b]	0.5[b]	45	-10[a]	-7.9[b]	-17.1[b]	-8.1
Reported international LUC factor (g CO_2e MJ^{-1})	15.6[c]	6.7[d]	—	7.1[e]	-1.3[f]	1.7[d]	—	2.2[e]	—
Biofuel shock size (GL ethanol y^{-1})	30	27			34	27			—
Energy crop yield (Mg ha^{-1} y^{-1})	15.1	10.1			~20	17.5			11.5[g]
Total direct land use (Mha)	5.1	9.5			10	5.1			—
Adjusted total induced LUC factor (Mg CO_2e ha^{-1} y^{-1})	1.7	0.16	0.53	0.03	3.3	-1.1	-0.89	-1.9	-0.57
Adjusted international LUC factor (Mg CO_2e ha^{-1} y^{-1})	1.9	0.40	—	0.42	-0.09	0.19	—	-0.24	—

[a]base-case estimate considered in Dunn *et al.* 2013 (25)

[b]average across the range of results reported

[c]estimated from Pavlenko & Searle 2018 (26), Figure 4 (LUC effects only)

[d]estimated from Pavlenko & Searle 2018 (26), Figure 7

[e]estimated from Qin *et al.* 2016 (22), Figure 5

[f]estimated from Pavlenko & Searle 2018 (26), Figure 9

[g]average for switchgrass and Miscanthus, across three assessment regions and two time periods (current and future)

Table S3. DayCent variables for NECB calculation.

NECB component	Intermediate carbon pool	DayCent output	DayCent output pool description (all in units of g C m^{-2})
Total above-ground C (AGC)	Aboveground live crop/grass C (AGL crop)	aglivc	Above ground live carbon for crop/grass
	Aboveground dead crop/grass C (AGD crop)	stdedc	Standing dead carbon for crop/grass
	Aboveground live forest C (AGL tree)	rleavc	Leaf live carbon for forest
		fbrchc	Fine branch live carbon for forest
		rlwodc	Large wood live carbon for forest
	Aboveground dead forest C (AGL tree)	wood1c	Dead fine branch carbon
		wood2c	Dead large wood carbon
	Surface litter	strucc(1)	Carbon in structural component of surface litter
		metabc(1)	Carbon in metabolic component of surface litter
Total below-ground C (BGC)	Belowground live crop/grass C (BGL crop)	bglivcj	Juvenile fine root live carbon for crop/grass
		bglivcm	Mature fine root live carbon for crop/grass
	Belowground live forest C (BGL tree)	crootc	Coarse root live carbon for forest
		frootcj	Juvenile fine root live carbon for forest
		frootcm	Mature fine root live carbon for forest
	Soil litter	strucc(2)	Carbon in structural component of soil litter
		metabc(2)	Carbon in metabolic component of soil litter
		wood3c	Dead coarse root carbon
	Soil organic matter	som1c(1)	Carbon in surface active soil organic matter
		som1c(2)	Carbon in soil active soil organic matter
		som2c(1)	Carbon in surface slow soil organic matter
		som2c(2)	Carbon in soil slow soil organic matter
		som3c	Carbon in passive soil organic matter

Table S4. Detailed ecosystem & biorefinery modeling results (30-year simulation averages).

Carbon pools for comparison	**Yield table column from reference (6), Appendix A**	**DayCent output name**	**DayCent pool description (all in units of g C m^{-2})**
Total living biomass C	live trees + understory vegetation (includes stems, branches, foliage, coarse roots)	rlwodc	Large wood live carbon for forest
		fbrchc	Fine branch live carbon for forest
		rleavc	Leaf live carbon for forest
		crootc	Coarse root live carbon for forest
Total dead biomass C	standing dead trees + down dead wood (includes stems, branches, foliage, coarse roots, and surface fuels)	wood1c	Dead fine branch carbon
		wood2c	Dead large wood carbon
Excluded	forest floor, soil organic carbon	All other DayCent C pools	

SI References

1. F. S. Chapin, *et al.*, Reconciling carbon-cycle concepts, terminology, and methods. *Ecosystems* **9**, 1041–1050 (2006).
2. G. M. Lovett, J. J. Cole, M. L. Pace, Is net ecosystem production equal to ecosystem carbon accumulation? *Ecosystems* **9**, 152–155 (2006).
3. J. L. Field, *et al.*, High-resolution techno–ecological modelling of a bioenergy landscape to identify climate mitigation opportunities in cellulosic ethanol production. *Nat. Energy* **3**, 211–219 (2018).
4. T. W. Hudiburg, B. E. Law, C. Wirth, S. Luyssaert, Regional carbon dioxide implications of forest bioenergy production. *Nature Climate Change* **1**, 419–423 (2011).
5. H. G. Lund, *Definitions of forest, deforestation, afforestation, and reforestation* (Forest Information Services, 2018). https://doi.org/10.13140/RG.2.2.31426.48323.
6. J. E. Smith, L. S. Heath, K. E. Skog, R. A. Birdsey, Methods for calculating forest ecosystem and harvested carbon with standard estimates for forest types of the United States (2006). http://www.treesearch.fs.fed.us/pubs/22954.
7. J. W. Veldman, *et al.*, Tyranny of trees in grassy biomes. *Science* **347**, 484–485 (2015).
8. N. Seddon, B. Turner, P. Berry, A. Chausson, C. A. J. Girardin, Grounding nature-based climate solutions in sound biodiversity science. *Nature Climate Change* **9**, 84 (2019).
9. G. Popkin, How much can forests fight climate change? *Nature* **565**, 280 (2019).
10. S. J. Del Grosso, W. J. Parton, C. A. Keough, M. Reyes-Fox, "Special features of the DayCent modeling package and additional procedures for parameterization, calibration, validation, and applications" in *Advances in Agricultural Systems Modeling*, Methods of introducing system models into agricultural research., L. R. Ahuja, L. Ma, Eds. (American Society of Agronomy, Crop Science Society of America, Soil Science Society of America, 2011), pp. 155–176.
11. X. Liu, T. Yang, Q. Wang, F. Huang, L. Li, Dynamics of soil carbon and nitrogen stocks after afforestation in arid and semi-arid regions: A meta-analysis. *Science of The Total Environment* **618**, 1658–1664 (2018).
12. L. Deng, Z. Shangguan, Afforestation drives soil carbon and nitrogen changes in China. *Land Degradation & Development* **28**, 151–165 (2017).
13. D. Li, S. Niu, Y. Luo, Global patterns of the dynamics of soil carbon and nitrogen stocks following afforestation: a meta-analysis. *New Phytologist* **195**, 172–181 (2012).
14. J. M. H. Knops, D. Tilman, Dynamics of soil nitrogen and carbon accumulation for 61 years after agricultural abandonment. *Ecology* **81**, 88–98 (2000).
15. E. A. Paul, S. J. Morris, J. Six, K. Paustian, E. G. Gregorich, Interpretation of soil carbon and nitrogen dynamics in agricultural and afforested soils. *Soil Science Society of America Journal* **67**, 1620–1628 (2003).
16. F. Mesinger, *et al.*, North American Regional Reanalysis. *Bulletin of the American Meteorological Society* **87**, 343–360 (2006).
17. M. Laser, H. Jin, K. Jayawardhana, L. R. Lynd, Coproduction of ethanol and power from switchgrass. *Biofuels, Bioproducts and Biorefining* **3**, 195–218 (2009).
18. U. S. Environmental Protection Agency, Assessment and Standards Division, Office of Transportation and Air Quality, Renewable fuel standard program (RFS2) regulatory impact analysis. *United States Environmental Protection Agency, Washington, DC* (2010). https://nepis.epa.gov/Exe/ZyPURL.cgi?Dockey=P1006DXP.TXT.

19. F. Taheripour, W. E. Tyner, M. Q. Wang, Global land use changes due to the US cellulosic biofuel program simulated with the GTAP model. *Argonne National Laboratory* (2011). https://greet.es.anl.gov/publication-luc_ethanol.

20. J. B. Dunn, S. Mueller, H. Kwon, M. Q. Wang, Land-use change and greenhouse gas emissions from corn and cellulosic ethanol. *Biotechnology for Biofuels* **6**, 51 (2013).

21. F. Taheripour, W. E. Tyner, Induced land use emissions due to first and second generation biofuels and uncertainty in land use emission factors. *Economics Research International* **2013**, 1–12 (2013).

22. Z. Qin, J. B. Dunn, H. Kwon, S. Mueller, M. M. Wander, Influence of spatially dependent, modeled soil carbon emission factors on life-cycle greenhouse gas emissions of corn and cellulosic ethanol. *GCB Bioenergy* **8**, 1136–1149 (2016).

23. R. Plevin, G. Mishra, Estimates of the land-use-change carbon intensity of ethanol from switchgrass and corn stover using the GCAM 4.0 model. *Report to Environmental Working Group* (2015). http://static.ewg.org/reports/2015/better-biofuels-ahead/plevinreport.pdf.

24. H. Valin, *et al.*, "The land use change impact of biofuels consumed in the EU: Quantification of area and greenhouse gas impacts" (2015). https://ec.europa.eu/energy/sites/ener/files/documents/Final Report_GLOBIOM_publication.pdf.

25. J. B. Dunn, *et al.*, "Supply chain sustainability analysis of three biofuel pathways" (Idaho National Laboratory (INL), 2013). http://www.osti.gov/scitech/biblio/1149014.

26. N. Pavlenko, S. Searle, "A comparison of induced land-use change emissions estimates from energy crops" (The International Council on Clean Transportation, 2018). https://theicct.org/publications/comparison-ILUC-emissions-estimates-energy-crops.